

VEGA: a new Visible spECTroGraph and polArimeter on the CHARA Array

D. Mourard^a, K. Perraut^b, D. Bonneau^a, J.M. Clause^a, Ph. Stee^a, I. Tallon-Bosc^c, P. Kervella^d, Y. Hughes^a, A. Marcotto^a, A. Blazit^a, O. Chesneau^a, A. Domiciano de Souza^e, R. Foy^c, F. Hénault^a, D. Mattei^e, G. Merlin^a, A. Roussel^a, M. Tallon^c, E. Thiebaut^c, H. McAlister^{f,g}, T. ten Brummelaar^g, J. Sturmann^g, L. Sturmann^g, N. Turner^g, C. Farrington^g and P.J. Goldfinger^g

^aOCA/UNS/CNRS FIZEAU Avenue Copernic, 06130 Grasse, France

^bUJF/CNRS LAOG BP53, 38041 Grenoble Cedex 9, France

^cUCBL/CNRS CRAL 9 avenue Charles André, 69561 Saint Genis Laval cedex, France

^dObservatoire de Paris LESIA, 92195 Meudon, France

^eOCA/UNS/CNRS FIZEAU Parc Valrose, 06108 Nice cedex 2, France

^fGeorgia State University, P.O. Box 3969, Atlanta GA 30302-3969, USA

^gThe CHARA Array, Mount Wilson Observatory, Mount Wilson CA-91023 ,USA

ABSTRACT

The VEGA spectrograph and polarimeter has been recently integrated on the visible beams of the CHARA¹ Array. With a spectral resolution up to 35000 and thanks to operation at visible wavelengths, VEGA brings unique capabilities in terms of spatial and spectral resolution to the CHARA Array. We will present the main characteristics of VEGA on CHARA, some results concerning the performance and a preliminary analysis of the first science run.

Keywords: Visible interferometry, CHARA, Spectroscopy

1. INTRODUCTION

Very High Angular Resolution in Astrophysics, i.e. well beyond the diffraction limit of monolithic telescopes, has recently known a historical step with the decommissioning of interferometers like GI2T,² IOTA³ or COAST⁴. The era of pioneers is now close and the great development of worldwide facilities like VLTI,⁵ KECK-I⁶ and CHARA¹ is now in progress. Although the visible domain has been recognized as one of the main goals of the future developments of optical interferometry, short wavelength operation is not foreseen on the VLTI for the second generation instruments or on the KECK-I.

VEGA^{7,8} (Visible spECTroGraph and polArimeter) is a visible focal instrument installed on the CHARA stellar interferometer located in Mt Wilson, CA. The long experience of our group and the good conditions of CHARA have permitted a very fast implementation of this new instrument. With 30000 of spectral resolution and baselines up to 330m, VEGA will help to finally realize CHARA's visible goals and propel this unique facility at the level of the interferometer with the world's largest spectral and spatial resolution. Its spectral and polarimetric characteristics make it very complementary to the others instruments, either the infrared ones such as CLASSIC,¹ FLUOR⁹ and MIRC¹⁰ or the new visible combiner under qualification PAVO¹¹.

Infrared and visible measurements are complementary for a correct and complete radiative transfer modeling. On one hand, many of the astrophysical processes involved in stellar physics and investigated by interferometry have stronger signatures at visible wavelengths. On the other hand, new physical processes will be investigated, broadening the field of astrophysical domains. The spatial resolution will reach the unequaled value of 0.3 millisecond of arc at 0.6 μm with the longest baseline. Moreover, the high spectral resolution will allow to study with unprecedented details the kinematics of stellar sources. Finally, the most promising science drivers, only

Further author information: (Send correspondence to D. Mourard)

D. Mourard: E-mail: Denis.Mourard@obs-azur.fr, Telephone: 33 493 405 365

Optical and Infrared Interferometry, edited by Markus Schöller, William C. Danchi, Françoise Delplancke
Proc. of SPIE Vol. 7013, 701323, (2008) · 0277-786X/08/\$18 · doi: 10.1117/12.787505

possible with this visible instrument, seem to be within the fields of fundamental stellar parameters, stellar activity (rotation, surface structures, polarization, pulsation) and circumstellar environments studies. It has been demonstrated¹² that the only way to reach stellar surface imaging for asteroseismology studies and to understand the relation between the interior and the environment of the stars is through visible interferometry with spectral and spatial characteristics like VEGA on CHARA.

VEGA is based on the visible spectrograph of the GI2T/REGAIN interferometer². For its CHARA implementation we have made the choice to focus the operation on the dispersed fringe mode with the currently available spectral resolution (from 1500 up to 30000) and the unique polarimetric capabilities (SPIN experiment¹³). While the instrument is able to manage four beams at the same time, its operation has started with 2T fringes because of real time processing issues as well as necessary improvements in the data reduction pipeline. The extension to 3 and 4T operation is foreseen in the coming year. It will multiply by a factor of 4 to 10 the scientific output of VEGA. It is also interesting to note that simultaneous visible and infrared operations are permitted on CHARA, either on separate programs (two sub arrays running in parallel) or on coordinated programs (visible beams and infrared beams feeding two instruments simultaneously).

2. TECHNICAL DESCRIPTION

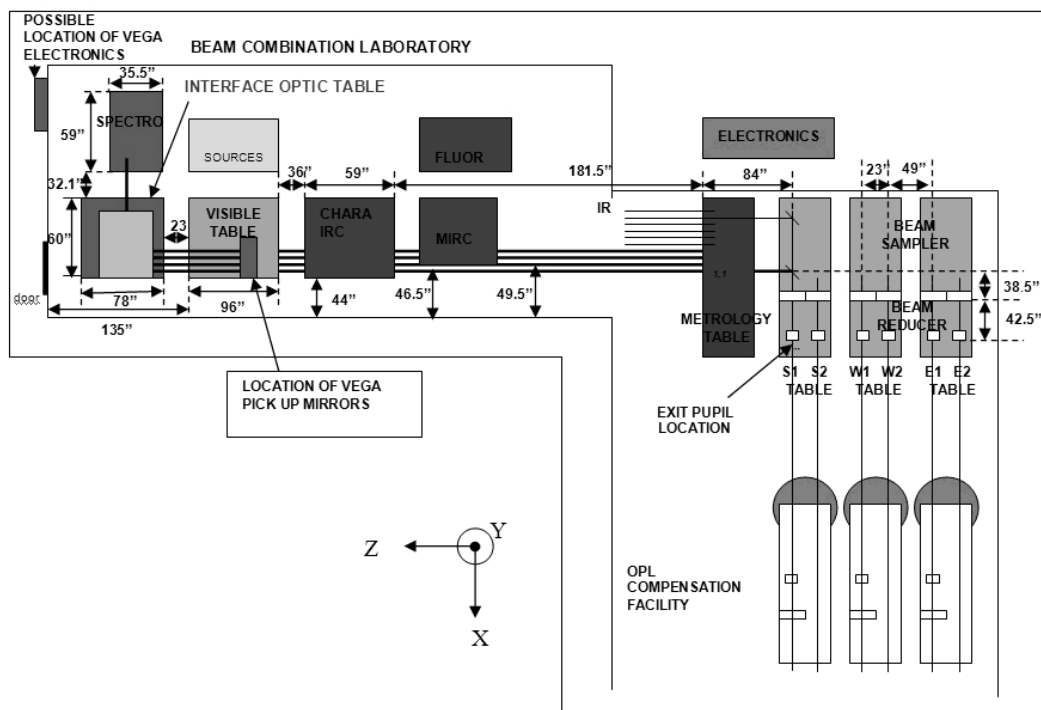


Figure 1. General implementation of VEGA in the CHARA optical lab. The VEGA instrument starts with the pickup mirrors installed on the CHARA visible table, where the CHARA beams are pick up and send to the VEGA Interface Optic Table and then to the spectrograph. The VEGA electronic cabinets are installed outside the lab. The instrument is operated from the CHARA control room, 100 meters away or from remote centers like the one installed in the Observatoire de la Côte d'Azur, France.

VEGA has been installed in the CHARA optical lab (Fig. 1) during a three-week run in September 2007. All the materials were shipped from France excepted some of the new subsystems (periscope, beam compressors) that have been manufactured by the CHARA workshops in Atlanta and Mount Wilson. The periscope and the VEGA Interface Optic Table subsystems (Fig. 2) perform the following tasks:

- geometrical adaptation of the beams: The CHARA collimated beams are 3/4 inch in diameter and horizontally distributed every 3 inches. The configuration of the VEGA spectrograph demands 4 collimated

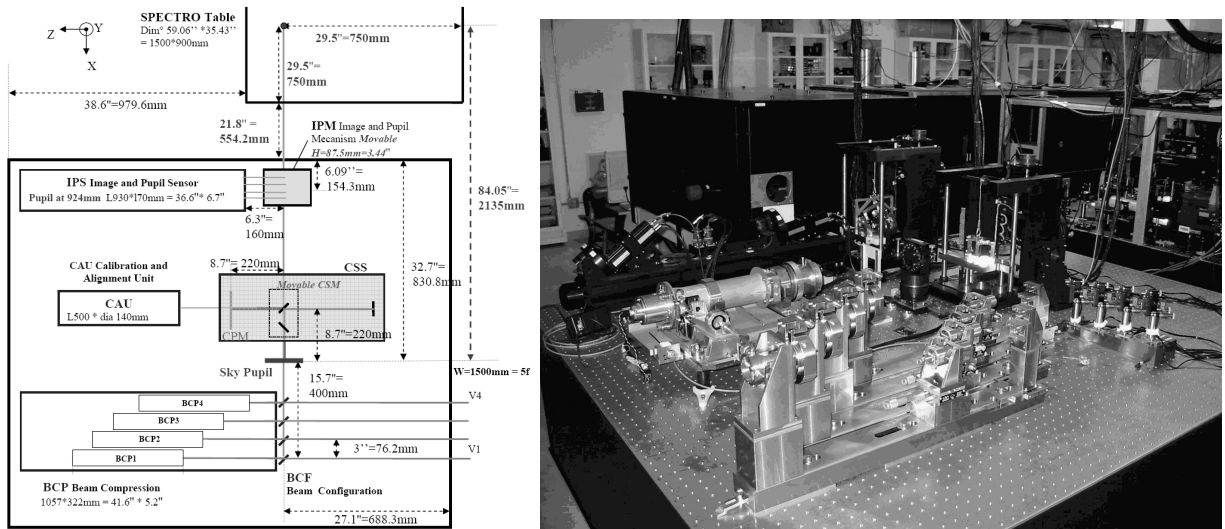


Figure 2. Optical layout (left) of the VEGA interface optical table and picture (right) of its installation in the CHARA optical lab. The two grey boxes on the layout (two black modules on the picture) represent two movable devices (CSM and IPM). The CSM (Calibration and Sources Module) allows to send the various sources simultaneously in the direction of the spectrograph and of CHARA, thanks to a beam splitter, a flat mirror and a compensating parallel plate. The IPM (Image and Pupil Module) in its bottom position sends the beam to the Image and Pupil Sensor, whereas in the upper position the beams are sent to the spectrograph.

beams, 5mm in diameter, vertically aligned and separated by 10mm center to center. This function is achieved on each beam by a set of 2 flat mirrors (M1 and M2) in the periscope, a 3-mirror asymmetrical cat's eye for the beam compressor and a flat mirror (M6) feeding the spectrograph. On each beam, two mirrors (M2 and M6) are equipped with picomotors allowing a fine and remote alignment between the VEGA reference beam and the CHARA reference position, both in direction and position.

- control of the longitudinal position of the CHARA pupils. Fresnel diffraction in the visible¹⁴ as well as a correct definition^{15, 16} of the energy supports in the spectral densities of the VEGA fringed images require a correct re-imaging of the CHARA pupils at the entrance of the spectrograph. The CHARA pupils in the optical lab are formed somewhere behind the secondary mirror of the Beam Reducing Telescope on the beam sampler tables (see Fig. 1). However the exact position depends on the POP configuration (fixed delay in the vacuum pipes) as well as on the current position of the delay line cart on the rails. Then the optical paths in the beam samplers being different from one line to another, the range of pupil distance at the entrance of the VEGA interface table could vary from 15 to 26m. By optimizing the distribution of lines on the beams we can reduce the range of variation to about 7m around a mean position of 20m. Thus the secondary mirrors of the VEGA beam compressors (each one installed on one fixed beam) have been adapted to a set of preferred lines so that at the output of the beam compressor, the pupil position can vary by about $\pm 150\text{mm}$ around a mean theoretical distance of 2135mm. This has been calculated to be acceptable with respect to visibility losses due to Fresnel diffraction effects.
- equalization of the internal optical paths. This is done by the different longitudinal positions of the beam compressors. By using successively a CHARA visible source and our VEGA visible source on the same corner cubes located for control purposes near the Beam Reducing Telescopes, we have been able to equalize the internal optical paths of VEGA to less than $100\mu\text{m}$ with respect to the CHARA reference positions.
- alignment and calibrations. Various sources (laser, spectral lamp, extended or point like white light source) can be projected towards the spectrograph and simultaneously to CHARA for alignment and calibration purposes. Just before being sent to the spectrograph, the four beams can be directed towards a reference device giving an image of the four image and pupil planes at the same time. This is used for alignment

control as well as for input data in the data reduction pipeline.

The VEGA spectrograph has already been described in various papers^{2,7}. The main improvement done for the CHARA implementation has been the renovation of the two photon counting detectors, now equipped with new generation of image intensifiers and with CMOS detectors allowing us to reach a Quantum Efficiency between 20 and 30%, depending on the wavelength and on the detector. More details could be found in Blazit et al.¹⁷.

Finally, the control of the VEGA instrument has been thought again to conform to the CHARA control system and to allow a remote operation of the observations. A detailed description of this control system is presented at this conference¹⁸. An important feature is the possibility of performing the group delay tracking by real time processing of the data and communications with the delay lines. The principle of this group delay tracking could be found in Koechlin et al¹⁹.

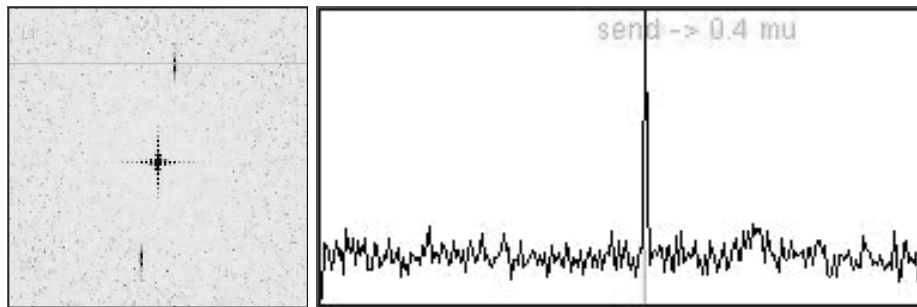


Figure 3. Screen captures of the VEGA group delay tracking system. Left: the integration of the 2D spectral densities of the $X - \lambda$ images showing the high frequency peak laterally shifted due to the optical path difference. For avoiding a possible corruption in the visibility measurement by the diffraction on the slit edges, the fringes are servo-controlled around a non null optical path difference. Right: a cut of the 2D spectral density where the fringe position is detected and the corresponding correction is calculated, taking into account the programmed fixed offset to tilt the fringes.

During the June 2008 VEGA observing run, the system has performed an efficient group delay tracking (see Fig. 3) with correction (signal to noise ratio larger than about 8) every 5 to 10 seconds by steps of less than $5\mu\text{m}$ on stars up to magnitude 6.4 in low spectral resolution, 5 in medium spectral resolution and 3.4 on high spectral resolution. The performance of the system depends on the seeing conditions as well as on the actual visibility of the observed object. However it has been noticed that in the high spectral resolution mode, due to the very large coherence length and to the good knowledge of the baseline, the fringes were moving very slowly, allowing the possibility for longer integration before reaching a decent signal to noise ratio on the optical path difference measurement. This may improve the limiting magnitude in this mode of about 1 magnitude.

3. PRINCIPLES OF THE VARIOUS OBSERVING MODES

3.1 The spectrograph characteristics

The spectrograph is designed to cover the visible band from 0.45 to 0.9 μm . It is equipped with two photon counting detectors looking simultaneously at two different spectral bands. The main characteristics are summarized in Table 1. The simultaneous operation of the two detectors is only possible in high and medium spectral resolution. The optical design has been calculated to allow the simultaneous recording, in medium spectral resolution, of the spectral region around $H\alpha$ on the red detector and around $H\beta$ on the blue detector.

The spectral calibrations are done before any change of the grating turret configuration (rotation or change of grating). They are performed at any time during the night by projecting into the spectrograph the light coming

Grating	R	$\Delta\lambda$ (Blue)	$\Delta\lambda$ (Red)	$\lambda_R - \lambda_B$
R1: 1800gr/mm	35000	4 nm	6 nm	25 nm
R2: 300gr/mm	5000	35 nm	50 nm	156 nm
R3: 100gr/mm	1700	105 nm	150 nm	not possible

Table 1. Spectral resolutions (R) and bandwidths ($\Delta\lambda$) of the VEGA spectrograph, as well as the spectral separation between the two detectors.

from a Thorium-Argon spectral lamp. The complete sequence of setting the system and recording the calibration data takes about 3 minutes. The calibration is made simultaneously on both detectors. Some examples of spectrum are shown on Fig. 4

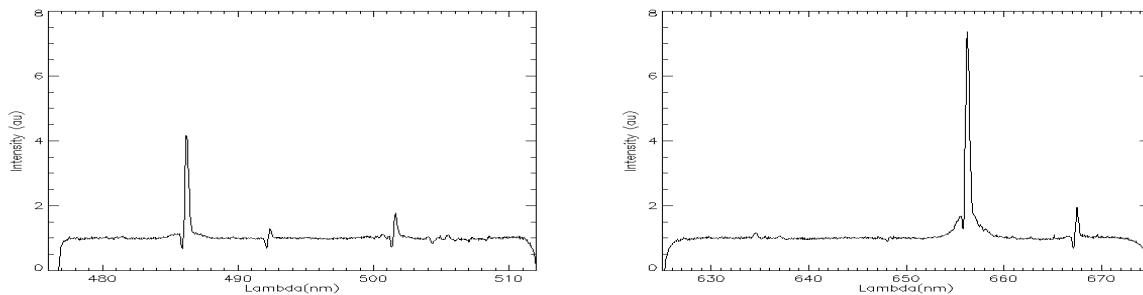


Figure 4. P Cygni spectrum around $H\beta$ (left) and $H\alpha$ (right) recorded simultaneously with the two photon counting detectors *ALGO LB* and *ALGO LR* during the June 2008 VEGA run (June 2th UT08:30).

3.2 The polarimetric mode

The GI2T/REGAIN interferometer was designed with a polarimetric mode inside its spectrograph and this module is now implemented in VEGA, which will thus provide spectro-polarimetry at sub-milliarcsecond (mas) angular resolution and allow mass-loss events from hot stars, inhomogeneous circumstellar materials or magnetic field topologies to be investigated.

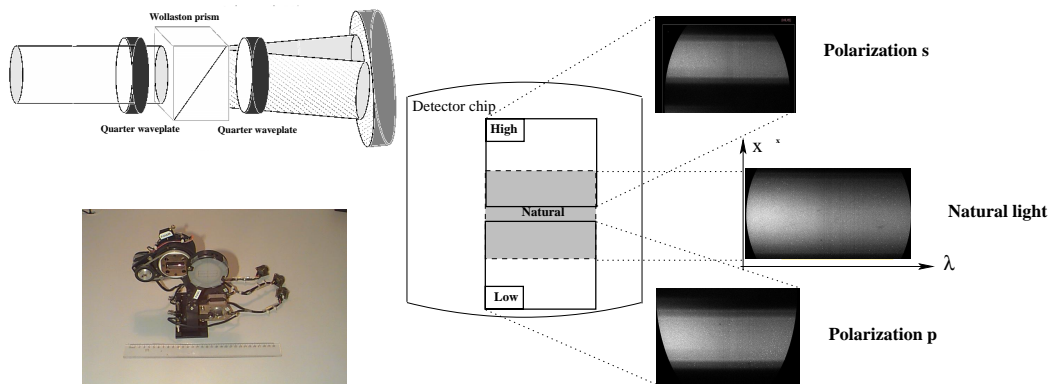


Figure 5. **Left:** Sketch (top) and front-view photograph (bottom) of the polarimetric mode included in VEGA. **Right:** (x, λ) images recorded on the red photon-counting detector for observations in polarized light (two simultaneous images *High* and *Low* corresponding to two perpendicular polarization directions) and in natural light (a single centered image).

The polarimeter, placed just before the spectrograph grating, is mainly composed of a Wollaston prism to separate two orthogonal polarization states and of a movable quarter waveplate (Figure 5). To avoid unbalanced transmissions of the polarization states by the grating, a fixed quarter waveplate is assembled after the Wollaston prism in the same mechanical mount to transform the two linearly polarized output beams in two circularly

polarized ones that are affected by the same throughput factor by the grating grooves. After being spectrally dispersed, the two beams carrying both the interference pattern and the polarization information are focused on the photon-counting detectors that contain two (x, λ) images, one per polarization state referred to as *High* and *Low* with respect to their position on the detector (Figure 5). As previously detailed,¹³ such a device gives access to interferometric observables in three (I , Q , and V) of the four Stokes parameters.

During the June 2008 VEGA observing run, we manage in observing with this polarimetric mode and in recording several series of polarized data sandwiched by observations in natural light. This mode operation is validated but the mode needs to be calibrated by observing, for each baseline, calibrators of various declinations throughout their observability range.

3.3 Multiple baseline operations.

As already said, four simultaneous beams can be accepted by the spectrograph optics. The optical configuration is presented on Fig. 6.

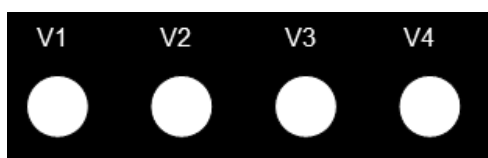


Figure 6. Configuration of the VEGA entrance pupil. At the entrance of the spectrograph these four beams are vertically aligned, with the beam V1 at the upper position.

For the first observing runs, it has been decided to operate VEGA in the 2T mode only, to simplify the data reduction pipeline. However an interesting capability of VEGA+CHARA is that with four telescopes and four delay lines tracking the star and fringes, it is very easy and fast to switch from one baseline to another. Indeed, between the CHARA tip/tilt sensor and the VEGA periscope, shutters are installed on each visible beam. It is thus possible to record data on baseline V1V2 or V2V3 or V3V4 by a simple configuration of the shutters. This operating mode has been successfully tested during the last VEGA observing run (June 2008) and it has been shown that it takes only about 3 minutes between the end of recording on one baseline and the start of recording on the second baseline. For this kind of observations (see Fig. 7) we have in fact used the capabilities of CHARA of running multiple sub arrays at the same time. One primary array was set on beams V1 and V2 (with for example V1 as the reference cart) and the secondary array was set on beams V3 and V4 (with V3 as the reference cart). Although it was in principle possible to record data on the third baseline V2V3 (with V3 as reference cart for V3V2 and for V3V4), this was not successfully attempted because of bad seeing conditions.

The next step is of course the operation with three or four telescopes simultaneously, opening access to a larger number of simultaneous measurements: 3 visibilities and 1 closure phase in the 3T mode or 6 visibilities and 3 closure phases in the 4T mode.

For the 3T mode we can use either the V1V2V4 or V1V3V4 configurations, depending on the used telescopes and the need for optimizing the pupil reimaging as already explained (see Sect. 2). These configurations correspond to a linear non-redundant arrangement of pupils well adapted to dispersed fringes. However it is obvious that the sampling of the V1V4 fringes and even the V1V3 or V2V4 fringes has to be checked carefully. Preliminary attempts with the internal white light source have shown that fringes on V1V3 or V2V4 are correctly detected with the same optical magnification in the spectrograph and the same spatial resolution for the photon centroiding, but that fringes on V1V4 were undetectable (about 2 pixels per fringe spacing). One simple solution will be to increase the optical magnification by a factor 2 and an optical solution has been found but should be implemented. The drawback of this solution is to reduce the spectral bandwidths by a factor of 2! A more complex solution will be to change the anamorphosis factor of the two cylindrical mirrors without changing their optical implementation. The optical study has shown that it is in principle possible by keeping the sum of their focal lengths but changing their ratio. However, this solution is really costly because of the new manufacturing of

cylindrical mirrors. The best solution currently under study is to increase the spatial resolution on the detectors by a factor of 2. It has been shown¹⁷ that a resolution of $\frac{1}{4}$ of pixels is possible but tests on actual data are necessary to check the consequences on the interferometric observables. These tests will be made soon on the current 2T data thanks to the already implemented principle of recording sub images of 5×5 pixels around each detected photons. Finally the real time implementation of sub pixel centroiding will be necessary for group delay tracking on the different baselines.

Concerning the 4T mode (V1V2V3V4), the same problems about sampling have to be considered. To solve the problem of the redundant linear configuration of the pupils (spatial frequency V1V2, V2V3 and V3V4 are identical, as well as V1V3 and V2V4), we will use the principle of the spatio-spectral encoding of fringes, already described.⁷ However a special configuration of the group delay tracking has to be implemented for controlling the optical path differences (OPD) on baselines V1V2, V2V3 and V3V4 with respecting also the fixed OPD offsets necessary to separate the signal of the different redundant baselines.

4. PRELIMINARY ESTIMATION OF PERFORMANCE

4.1 Observing efficiency

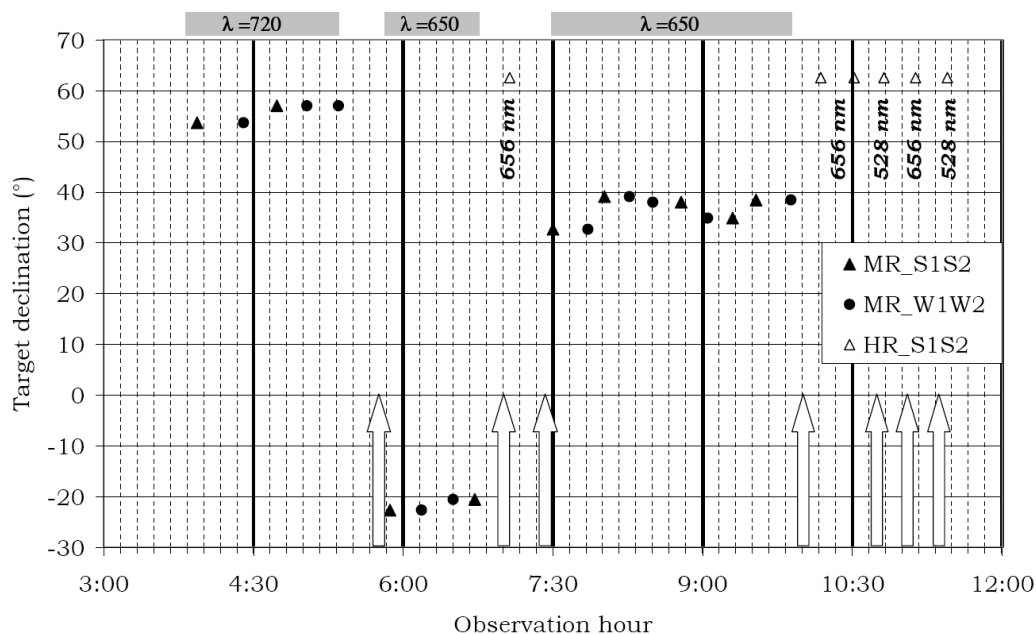


Figure 7. Example of the observation sequences for the night of June, 2nd with VEGA. 10 objects have been observed on two different baselines (S1S2 and W1W2). Various spectral modes have been used : medium resolution (MR) and high resolution (HR) for different central wavelengths (528 nm, 650 nm, 656 nm and 720 nm). Vertical arrows represent the associated spectral calibrations.

During the June 2008 VEGA run, we have shown that a baseline change can be performed within 3 minutes, by using shutter mode for the moment, which opened the opportunity of quasi-simultaneous observations on two different baselines. An observation sequence lasts about 15 minutes (for 10 files of 2000 images). Time to change of target and/or baseline does not exceed a few minutes since pointing the CHARA telescopes and finding fringes with VEGA are almost immediate as soon as the OPD offsets of the configuration are known. Sequences of a few minutes have to be added for spectral calibrations as soon as wavelength and/or spectral resolution are modified. As illustrated in Fig. 7, during the night of June, 2nd 10 different sources (targets and calibrators) have been observed; observations succeed to each other every 15 minutes while an integration takes about 10 minutes. Overheads between each observation (pointing, pupil and image check, optimization of the camera gains, fringe search) are thus very short.

Note that for the polarimetric mode,¹³ some optimization can be implemented to gain time since recording images and pupils after each step is not mandatory.

4.2 Comparison of measured performance with estimations

In multimode operation, we usually consider two domains for the signal to noise ratio, depending on the number of photons per speckle per single exposure. If this number is larger than 1, then the signal to noise ratio increases as the square root of the number of photons, whereas if it is smaller than 1, the signal to noise ratio increases as the number of photons.²⁰ As a consequence, we define the limiting magnitude as the magnitude giving 1 photon per speckle per single exposure. It is clear however that the signal to noise ratio could reach high values at this limit, since one can integrate a large number of single exposures containing a large number of speckles. In the differential regime, it has been shown,²¹ that the signal to noise ratio is the geometrical mean of the signal to noise ratios in the reference channel and in the science channel. We have used these hypothesis for the initial performance estimations of VEGA.⁷ In the present paper we have adapted the parameters of the simulation to correctly reproduce what has been observed on the sky during the last VEGA observing run in June 2008. The data are presented on Table 2. We also take into account the effective operating cycle of the detectors, i.e. 40 frames per second, each frame being exposed during 15ms.

mV	$\Delta\lambda$ (nm)	λ (nm)	V^2	Integ. Time (s)	r_0 (cm)	SNR
3.4	5 nm	650 nm	1.0	10	12	10
4.9	40 nm	650 nm	0.4	10	15	20
6.4	50 nm	650 nm	0.5	10	6	5

Table 2. First measurements of performance on VEGA+CHARA

From these values and by comparison to the previous simulations we can estimate some raw numbers on the transmission and on the instrumental visibility. On the basis of the previous calculations we have found that the instrumental V^2 visibility should be around 0.7 to 0.8. The global transmission is estimated to 0.1%, with 5% for CHARA, 13% for VEGA and 18% for the detector (including its duty cycle). We have also established a lower limit for the VEGA operation when r_0 is below about 5 cm.

4.3 Limiting performance

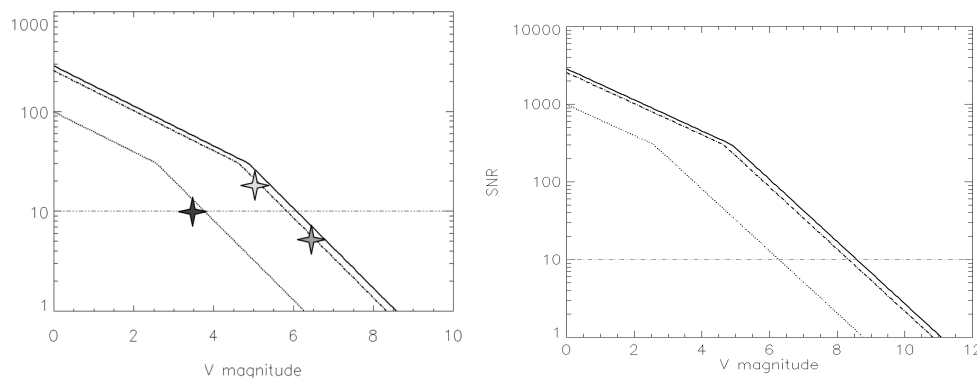


Figure 8. Left: VEGA signal to noise ratio for a 10s integration. The three symbols represent the measurements presented in Table 2 (from left to right: high, medium and low spectral resolution). Right: VEGA signal to noise ratio for a 1000s integration. In both figures, the dotted line is for the high spectral resolution mode ($\Delta\lambda = 6nm$), the dashed one for the medium resolution mode ($\Delta\lambda = 40nm$) and the solid line for the low resolution mode ($\Delta\lambda = 50nm$ due to the spectral decorrelation of the atmospheric turbulence). We use the median seeing value ($r_0 = 8cm$) and the transmission estimated in the previous section.

The results of the previous section permit us to estimate the limiting performances of VEGA+CHARA in the various spectral resolution modes. We have considered two main cases for the simulation: the current one

(Fig. 8, left) where VEGA should do its own group delay tracking in about 10s for correcting the slow optical path difference variations, then the case (Fig. 8, right) where an external fringe tracker (as CHAMP²²) will be in operation and allow long integrations on VEGA (typically 30mn of time). The parameters of the simulation have been adapted to correctly reproduce the measurements presented in Table 2. During the first observations in low resolution mode, it was noted that if one takes the whole spectral band for the fringe tracking (150nm) then the fringe contrast is very low due to the spectral decorrelation of the atmosphere²³ and the correct operation requires to limit the spectral band to about one third of this band.

4.4 Preliminary analysis of data

During the June 2008 VEGA run, the scientific programs that have been started concern mainly the three following points:

1. V^2 , differential phase and polarimetric mode qualification,
2. Fast rotators (α Cep, δ Aql),
3. Emission line stars (β Lyr, ν Sgr, δ Sco, ζ Oph, P Cyg).

For the first program on the V^2 qualification, it has been necessary to solve a few issues on the data reduction pipeline. The three main problems were the bad quality of the pupil images, some vibrations on one of the reference delay lines and some residual cosmetic problems on the detector. These issues are now solved but we are not able to present results at that time.

The polarization qualification program was not completely successful because of poor seeing conditions. However, the preliminary analysis that have been made show that the observing procedure is now correctly established.

For the qualification of the differential phase measurements, we have recorded data in the high spectral resolution mode in two continuum regions of α Cep on the S1S2 baseline. The main purpose of this qualification was to estimate the raw variance of the phase measurements and to identify some chromatic effects that may be introduced by the instrument or the atmosphere. The results are presented in Fig. 9. We found a variance of about 3° , which corresponds to an astrometric precision of about 40 microseconds of arc. However we can notice some smooth variations that could be interpreted as effects of the atmospheric dispersion and that could be easily removed by polynomial adjustments.

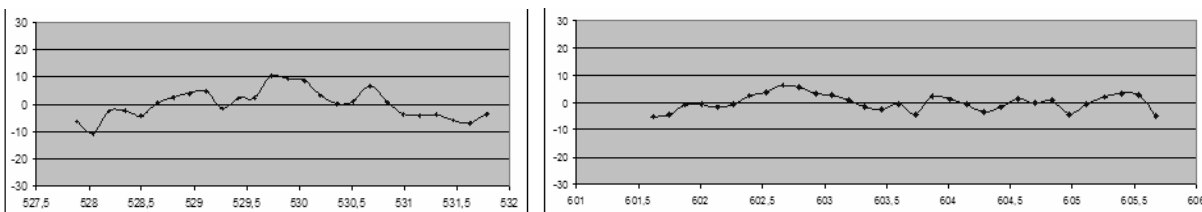


Figure 9. Differential phase measurements in two continuum regions of α Cep. Left: spectral band centered around 530nm. Right: spectral band centered around 604nm. In the first case the variance of the residual is about 5° , whereas it goes down to 3° in the second case. For the S1S2 baseline used in these measurements, it corresponds to an astrometric precision of about 40 microseconds of arc.

5. SUMMARY OF THE MAIN SCIENTIFIC PROGRAMS UNDER INVESTIGATION

5.1 Stellar differential rotation from spectro-interferometry

In this section we show how spectro-interferometry can be used to measure differential rotation on stellar surfaces. The results and formalism presented here are based on the work from Domiciano de Souza et al.²⁴ First measurements have been obtained during the June 2008 VEGA run on the stars α Cep and δ Aql.

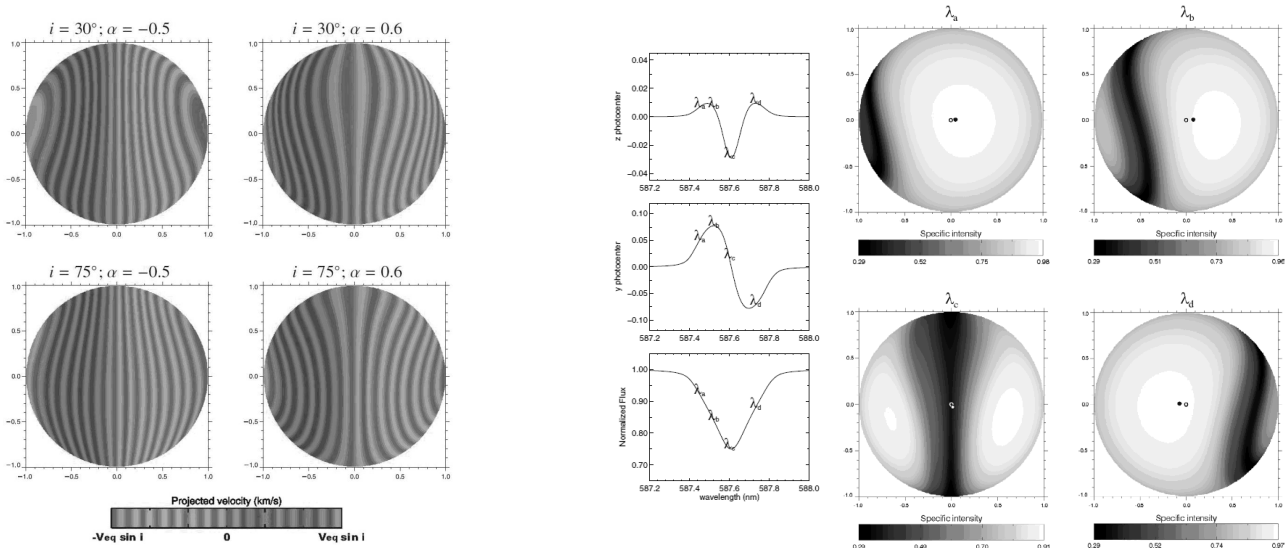


Figure 10. Left: Radial velocity maps for several combinations of polar inclination i and differential rotation parameter $\alpha = (\Omega_{\text{eq}} - \Omega_{\text{p}})/\Omega_{\text{eq}}$ (assuming a solar-like differential rotation law). A positive velocity corresponds to displacements towards the observer (blue shifts). For differential rotation, regions of constant projected velocity (equal velocity strips) are not straight vertical ones as it is the case for rigid rotation ($\alpha = 0$).

Right: Photocenter components, ϵ_z (top) and ϵ_y (middle), and the normalized spectral flux (bottom) across the asymmetric He I $\lambda 5876$ line. The calculations were performed for $v_{\text{eq}} \sin i = 100$ km/s, $\log g = 4.0$, $T_{\text{eff}} = 20\,000$ K, $i = 45^\circ$, and $\alpha = 0.6$. Photocenter components are given in units of angular stellar radius ρ . The letters indicate selected wavelengths corresponding to a region in the blue line wing (λ_a), the highest ϵ_y value (λ_b), the central wavelength (λ_c), and the most positive value of ϵ_z (λ_d). The intensity maps associated to the DI observables are also shown for the four selected wavelengths. The curved dark patterns correspond to Doppler shifts of the local line profile caused by differential rotation.

Because of the differential rotation the maps of rotational velocity projected onto the observer's direction (v_{proj}) take the form of curved lines instead of the usual vertical straight lines found for uniform rotation. Some examples of these radial velocity maps are shown in Fig. 10 left where one can see that they are functions of both α (the differential rotation parameter) and of the polar inclination i . The curved radial velocity maps induced by differential rotation influence the photospheric line profile as well as the photocenter position as a function of the wavelength λ . Figure 10 right shows some examples of intensity maps at selected wavelengths inside a photospheric line for a differentially rotating star together with the spectral line and the photocenter components. Differential rotation changes the spectral profile and the photocenter components ϵ_y and ϵ_z . In particular we have $\epsilon_z(\lambda) \neq 0$, contrarily to the uniform rotation case where this quantity is always equal to zero (because the radial velocity maps take the form of vertical strips).

From these spectro-interferometric signatures of differential rotation one can in principle determine and disentangle the differential rotation parameter from the stellar inclination. Depending on the attained precision in the differential phase, the recent CHARA/VEGA observations should allow us to calibrate and validate this method to measure surface differential stellar rotation.

5.2 A long-term follow up of the Be star δ Scorpii disk formation with VEGA

δ Scorpii is one of the closest Be star of the southern hemisphere ($D = 123$ pc), one of the brightest and one of the most active ones. Thus its circumstellar environment can be almost fully resolved with baselines around 107 meters, as W1W2, (see Fig. 11). Using baselines from 33 (S1S2) to 107 meters we can study the disk morphology and determine some geometrical parameters (the equatorial disk size, the inclination angle, the presence of an extension in the polar wind, flux ratio between the equatorial disk and the polar wind). As the equatorial disk seems to be still forming, mass transfer between the photosphere and the circumstellar environment can be studied and, only long-term interferometric follow up observations can evidence the large visibility differences between the two possible scenarios.

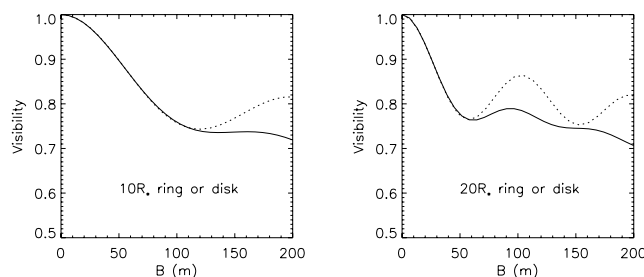


Figure 11. Visibilities from a toy model of a $10 R_{\star}$ (left) and $20 R_{\star}$ (right) uniform disk model in contact with the central star (solid line) versus a uniform ring (dotted line) with the same extension but starting at $1 R_{\star}$. from the central star assuming that for each case 20% of the flux in the visible is coming from the disk

δ Scorpii is also a well-known non-eclipsing binary system with a ~ 1.5 mag optically fainter companion with the orbital period of 10.6 years⁷ and a highly eccentric orbit ($e=0.94$ ⁷). The entire system is well within the field of view of the CHARA Telescopes (250 mas), the small magnitude difference between the two companions must modulate the interferometric signal, and thus it must be possible to resolve/confirm the binarity interferometrically, even if the disk may increase the brightness difference between the primary+disk and the secondary. Moreover, the next periastron, which will occur in 2011, may exhibit very interesting effects of the Be phenomenon. For instance, the close companion's proximity may trigger the disk formation/destruction.

The main goals of these observations are the following (by priority) to follow the disk formation as a function of time (between 2008 and 2012), to clarify one of the disk formation mechanisms (massive outburst, succession of small outbursts, slowly variable mass-loss, or persistent mass-loss), to constrain the disk geometry : extension, flattening, sharpness of the edge, to put some constraints on the putative polar wind (extension, opening angle, emission ratio between the polar wind and the equatorial disk) and finally to resolve the binary.

5.3 The wind activity of massive supergiants

The radiative winds of hot, massive stars are intrinsically unstable and continuously variable on various time scales. They are also sensitive to many perturbations occurring close to the stellar surface. Consequently, detecting and monitoring the perturbations of these outflows is a mean to probe the launching of the material. The discovery of patterned variability in the stellar winds of luminous hot stars is a serious hint that deep seated and localized perturbations arise close to the surface. However we should also investigate whether the period of the events is the period of rotation or the period of a moving pattern on the surface related, for example, to Non-Radial Pulsations. OB supergiants are better suited targets for spatially resolving the structure in their vicinity and monitor them: they are bright, more extended than main sequence stars, their rotation period is longer and their lower gravity makes their wind probably more sensitive to photospheric perturbations. Rigel (B8Ia, 2.75mas , $V=0.1$) has been extensively spectroscopically studied in the visible by A. Kaufer and co-workers.²⁵ They detected $H\alpha$ activity on a monthly timescale. Rigel was monitored over more than 4 months in 2006 and 2007, in the $\text{Br}\gamma$ line with AMBER using the $R=12000$ resolution (Chesneau, O. these proceedings). Rigel is also better studied in the $H\alpha$ line, and the $R=35000$ spectral resolution of VEGA is well suited, provided that the baselines for these observations are short enough. Many OB supergiant, with magnitudes ranging from $V=0$ to $V=3.5$ can potentially be observed with that resolution and the long baselines of CHARA are well suited for the study of these bright but compact sources. In particular, the detection of a (weak) magnetic field in ζ Orionis (O9Ib, $V=1.8$, 0.47mas) is a new step in this field.²⁶ This detection will allow to phase the activity in the $H\alpha$ line with the rotation of the star, and to prepare the interferometric observations.

6. CONCLUSIONS

We have presented the main characteristics of the VEGA spectrograph installed on the CHARA array. Preliminary results from the first observing run help to fix the expected performances and to show the main limitations. At that time, some efforts have to be put on the data processing pipeline, especially to take into account the

cosmetics of the new photon counting detectors and the actual shape of the CHARA pupils.

In the coming months, our plans are to validate the three/four telescopes mode of VEGA and to perform the first visible and infrared simultaneous observations. The possibility of the remote operation of VEGA will also be used to optimize the scientific return.

ACKNOWLEDGMENTS

We wish to greatly thank the various sources of funding that have permitted the good and rapid development of the VEGA project: Observatoire de la Côte d'Azur, the CHARA Array, the French astronomical agency INSU and the programs PNPS (stellar physics) and ASHRA (high angular resolution) from CNRS.

REFERENCES

- [1] ten Brummelaar, T., Mc Alister, H. et al., *ApJ* 628, 453-465, (2005)
- [2] Mourard D., Thureau N., Abe L. et al., *C.R.Acad.Sci. Paris*, t2, S. IV, p 35-44, (2001)
- [3] Traub, W. A., Ahearn, A., Carleton, N. P., et al. 2003, in *Interferometry for Optical Astronomy II*. Edited by Wesley A. Traub. *Proceedings of the SPIE*, Volume 4838, pp. 45-52 (2003)
- [4] J. E. Baldwin, C. A. Haniff, C. D. Mackay, and P. J. Warner. Closure phase in high-resolution optical imaging. *Nature*, 320, 595-597, (1986).
- [5] A. Glindemann et al., "VLTI technical advances present and future", *SPIE Proc* 5491, Glasgow (2004)
- [6] M. Colavita et al., *SPIE* 6268, Orlando (2006)
- [7] Mourard D., Bonneau D., Clause J.M. et al., *SPIE* 6268, Orlando (2006)
- [8] Stee Ph., Mourard D., Bonneau D. et al., *SPIE* 6268, Orlando (2006)
- [9] V. Coude du Foresto, P. Borde, A. Merand et al., *SPIE* 4838, 280, (2003)
- [10] J. Monnier et al. these proceedings (2008)
- [11] M. Ireland et al., these proceedings (2008)
- [12] S. Jankov, F. Vakili, A. D. de Souza and Janot Pacheco, E., *A&A*, 377, 721, (2001)
- [13] Rousselet-Perraut K., Le Bouquin J.B., Mourard D. et al., *A&A*, 451, 1133-1137, (2006)
- [14] Mékarnia D. and Gay J., *J. Opt.* 20 131-140, (1989)
- [15] Bério P., Mourard D., Chesneau O. et al., *JOSA-A* Vol.16 (1999)
- [16] Bério P., Mourard D., Pierron M. et al., *JOSA-A* Vol.18, (2001)
- [17] Blazit A., Rondeau X., Thiébaud E. et al., *Appl. Opt.* 47, 8, pp 1141-1151, (2008)
- [18] Clause J.M., these proceedings (2008)
- [19] Koechlin L., Lawson P.R., Mourard D. et al., *Appl. Opt.* 35, 3002-3009, (1996)
- [20] Roddier F., *Physics Report*, vol. 170, (1988)
- [21] Petrov R., Roddier F. and Aime C., *JOSA-A*, Vol. 3, (1986)
- [22] Berger D. et al., these proceedings (2008)
- [23] Bério P., Mourard D., Vakili F. et al., *JOSA-A* Vol.14, (1997)
- [24] Domiciano de Souza, A., Zorec, J., Jankov, S., et al., *A&A*, 418, 781 (2004)
- [25] Kaufer, A., Stahl, O., Wolf, B., et al., & Szeifert, T. *A&A*, 305, 887, (1986)
- [26] Bouret, J.C., Donati, J. F., Martins, F. et al., *ArXiv e-prints*, 806, arXiv:0806.2162 (2008)